

**$\beta$  decay of  ${}^6\text{He}$  into the  $\alpha + d$  continuum**

M. Pfützner,<sup>1</sup> W. Dominik,<sup>1</sup> Z. Janas,<sup>1</sup> C. Mazzocchi,<sup>1</sup> M. Pomorski,<sup>1</sup> A. A. Bezbakh,<sup>2</sup> M. J. G. Borge,<sup>3,4</sup> K. Chrapkiewicz,<sup>1</sup> V. Chudoba,<sup>2</sup> R. Frederickx,<sup>5</sup> G. Kamiński,<sup>2,6</sup> M. Kowalska,<sup>4</sup> S. Krupko,<sup>2</sup> M. Kuich,<sup>1,7</sup> J. Kurcewicz,<sup>4</sup> A. A. Lis,<sup>1</sup> M. V. Lund,<sup>8</sup> K. Miernik,<sup>1,9</sup> J. Perkowski,<sup>10</sup> R. Raabe,<sup>5</sup> G. Randisi,<sup>5</sup> K. Riisager,<sup>8</sup> S. Sambri,<sup>5</sup> O. Tengblad,<sup>3</sup> and F. Wenander<sup>4</sup>

<sup>1</sup>*Faculty of Physics, University of Warsaw, Pasteura 5, 02-093 Warszawa, Poland*

<sup>2</sup>*Joint Institute for Nuclear Research, 141980 Dubna, Moscow Region, Russia*

<sup>3</sup>*Instituto de Estructura de la Materia, CSIC, E-28006 Madrid, Spain*

<sup>4</sup>*ISOLDE, CERN, CH-1211 Geneva 23, Switzerland*

<sup>5</sup>*KU Leuven, Instituut voor Kern- en Stralingsfysica, 3001 Leuven, Belgium*

<sup>6</sup>*Institute of Nuclear Physics PAN, 31-342 Kraków, Poland*

<sup>7</sup>*Faculty of Physics, Warsaw University of Technology, 00-662 Warszawa, Poland*

<sup>8</sup>*Department of Physics and Astronomy, Aarhus University, DK-8000 Aarhus C, Denmark*

<sup>9</sup>*Physics Division, Oak Ridge National Laboratory, Oak Ridge, Tennessee 37831, USA*

<sup>10</sup>*Faculty of Physics and Applied Computer Science, University of Łódź, 90-236 Łódź, Poland*

(Received 10 June 2015; published 23 July 2015)

The rare  $\beta$ -decay channel of  ${}^6\text{He}$  into the  $\alpha + d$  continuum was investigated at the REX-ISOLDE facility. Bunches of postaccelerated  ${}^6\text{He}$  ions were implanted into the optical time projection chamber (OTPC), where the decays with emission of charged particles were recorded. This novel technique allowed us to extend the low-energy end of the spectrum down to 150 keV in  $\alpha + d$  center of mass, corresponding to a deuteron energy of 100 keV. The branching ratio for this process amounts to  $[2.78 \pm 0.07(\text{stat}) \pm 0.17(\text{sys})] \times 10^{-6}$ . The shape of the spectrum is found to be in a good agreement with a three-body model, while the total intensity is about 20% larger than the predicted one.

DOI: [10.1103/PhysRevC.92.014316](https://doi.org/10.1103/PhysRevC.92.014316)

PACS number(s): 23.40.Hc, 27.20.+n, 29.40.Cs

**I. INTRODUCTION**

The physics of nuclear halo continues to be an active research field in low-energy nuclear physics [1]. The key features of the halo, such as the possibility of factorization of the wave function into a core and a halo component, or the large spatial extension of the system with a large probability of tunneling into classically forbidden regions, simplify the description of many-body systems on the one hand, and are responsible for a rich spectrum of new phenomena on the other hand [2]. Most experimental information to date on the nuclear halo has been obtained by a broad range of nuclear reactions. Nevertheless,  $\beta$  decay offers a specific and sensitive method to address halo properties, which is not yet fully exploited [1]. One of the intriguing processes expected to shed light on the two-neutron halo structure is the  $\beta$ -delayed deuteron emission ( $\beta d$ ). It is believed to represent a decoupled halo decay, where the two neutrons transform into a deuteron in the periphery of the initial system, directly to the continuum. The branching ratio of this process and the shape of the energy spectrum of the emitted particles are very sensitive to details of the wave function of the initial state and to the interaction between the deuteron and the core in the final state. To date such a decay has been observed only in two cases:  ${}^6\text{He}$  [3] and  ${}^{11}\text{Li}$  [4].

The ground state of  ${}^6\text{He}$  decays predominantly by a Gamow-Teller transition to the ground state of  ${}^6\text{Li}$  with decay energy  $Q = 3.508$  MeV and half life of  $T_{1/2} = 807$  ms [5]. The decay channel into  $\alpha + d$  is energetically allowed with  $Q_{\beta d} = 2.033$  MeV. The spectrum of the sum of kinetic energies of both emitted particles in their center-of-mass frame is continuous with the maximum value equal to  $Q_{\beta d}$ .

The  $\beta d$  channel in  ${}^6\text{He}$  has been studied several times in the last 25 years. In the very first experiment at ISOLDE the branching ratio for the delayed emission of deuterons with energy larger than 250 keV was measured to be  $(2.8 \pm 0.5) \times 10^{-6}$  [3]. In a subsequent experiment in the same laboratory a larger branching ratio of  $(7.6 \pm 0.6) \times 10^{-6}$  for the deuteron energy larger than about 360 keV was claimed [6]. Later, a measurement performed at the TRIUMF facility by Anthony *et al.* [7] reported a much lower value of  $(1.8 \pm 0.9) \times 10^{-6}$  for the same deuteron energy threshold. The large error of the total intensity reflected uncertainties in the efficiency of the detection setup. The collected statistic, however, was much larger than in the previous experiments, which resulted in a precise determination of the shape of the spectrum. Finally, the most recent measurement of the  $\beta d$  channel in  ${}^6\text{He}$  was done at the Cyclotron Research Centre at Louvain-la-Neuve by Raabe *et al.* [8]. For the first time, the postaccelerated ions of  ${}^6\text{He}$  were implanted into a highly segmented silicon detector, which allowed counting of the incoming ions and thus provided precise absolute normalization. This yielded the most precise value for the branching ratio of  $(1.65 \pm 0.10) \times 10^{-6}$  for the deuteron energy above 350 keV [8], which agrees within error bars with the value reported by Anthony *et al.* [7]. In addition, the shape of the spectrum measured in Ref. [8], although

having smaller statistics, agreed very well with the shape determined in Ref. [7]. All mentioned experiments suffered from the huge background due to  $\beta$  electrons emitted in the main decay channel of  ${}^6\text{He}$ . This background plagued the low-energy part of the spectrum and was the main reason why it was impossible to measure deuterons with energy below 350 keV.

Despite variations and inaccuracies of the reported values of the branching ratio for the  $\beta d$  channel in  ${}^6\text{He}$ , its order of magnitude,  $10^{-6}$ , was correctly established in the first experiments and at that time it was found puzzling. The early theoretical predictions for this branching ratio, based on various models, ranged between  $3 \times 10^{-5}$  and  $10^{-4}$  [3,9,10]. Later it was understood that the very small value of this branching ratio results from the cancellation of the internal and the external parts of the overlap between the  ${}^6\text{He}$  ground state and the  $\alpha + d$  scattering wave functions in the Gamow-Teller matrix element [11–14]. This conclusion is confirmed by the most recent theoretical description of the  $\beta d$  decay of  ${}^6\text{He}$ , which employs the  $\alpha + n + n$  three-body wave function in hyperspherical coordinates for  ${}^6\text{He}$  and a potential model for the  $\alpha + d$  scattering states [15]. The cancellation effect was found to be very sensitive to the details of the initial and the final states providing an efficient probe for both of them. In addition, the theoretical spectra suggested that about 30% of the intensity of the deuteron spectrum resides at lower energy, in the region not yet accessed by experiment. Thus, extending the measurement of  ${}^6\text{He}$   $\beta d$  spectrum to lower energies might provide a more stringent test of theoretical models and improve our understanding of the  ${}^6\text{He}$  halo structure.

Motivated by this challenge, we have attempted to measure low-energy deuterons emitted in the  $\beta d$  decay of  ${}^6\text{He}$ . To accomplish this we have applied a novel technique employing a gaseous time projection chamber, which allows recording and reconstructing tracks of  $\alpha$  particles and deuterons while being much less sensitive to  $\beta$  electrons. Here we report on results of this experiment in which we succeeded to extend the  $\beta d$  spectrum down to the deuteron energy of 100 keV.

## II. EXPERIMENTAL TECHNIQUES

Ions of  ${}^6\text{He}$  were produced at the CERN-ISOLDE facility by a 1.4 GeV proton beam impinging on a  $\text{UC}_x$  target. On average, the proton pulses were arriving every 3.2 s over the total measuring time, which amounted to 4.4 days. The reaction products, diffusing out of the target, were ionized in the versatile arc discharge ion source (VADIS) to  $1^+$  charge state. After extraction, mass-six ions were selected by the GPS mass separator. With the transport optimised for the  ${}^6\text{He}$  ions, most of the contaminant  ${}^6\text{Li}$  was removed from the beam. Then, the ions were directed into the REX-ISOLDE facility where they were bunched, charge bred to the  $2^+$  charge state, and postaccelerated to 3 MeV/nucleon [16]. A stripper foil was used to further eliminate  ${}^6\text{Li}$  and  ${}^{12}\text{C}$  contaminants, the latter originating in the breeder. After each proton impact on the ISOLDE target, REX-ISOLDE delivered  ${}^6\text{He}$  ions structured into the three approximately 20  $\mu\text{s}$  long macrobunches separated by 50 ms. These three macrobunches

contained, on average,  $10^4$  ions of  ${}^6\text{He}$  in total, which were delivered to the detection station.

The decay of  ${}^6\text{He}$  ions was measured by the gaseous optical time projection chamber (OTPC). This detector, developed at the University of Warsaw, was designed to study very rare decays with emission of charged particles, such as two-proton radioactivity [17,18], or  $\beta$ -delayed multiparticle emission [19,20]. Here we present briefly the principle of its operation and details specific to the present experiment. More information is given in Ref. [18], where the same detector unit is described. The active volume of the chamber, of 31 cm length, 18 cm width, and 21 cm height, was filled by a gas mixture of 98% He and 2%  $\text{N}_2$  at atmospheric pressure. Within this volume a constant and uniform electric field of 210 V/cm was maintained. Ions of interest enter the detector through a kapton entrance window and are stopped inside the active volume. Ions and charged particles emitted in the decay ionize the gas. The primary ionization electrons drift in the electric field with a constant velocity  $v_d$  towards the charge multiplication stage composed of four GEM foils [21] and a wire mesh anode. Electrons arriving at the anode stimulate atoms of the gas mixture to emit light. In contrast to traditional TPC detectors, which detect the final signal by electronic means, the OTPC operates by recording the emitted light. This is accomplished by a CCD digital camera and a photomultiplier (PMT) connected to a digital oscilloscope. The CCD image of  $512 \times 512$  16-bit pixels represents a projection of a particle track on the anode plane, integrated over the exposure time. The waveform of the PMT signal represents the total light intensity as a function of time. It provides information on the sequence of events within the exposure time and on the vertical projection of particles tracks. By combining the data from the CCD image and the PMT waveform one can reconstruct the track of a charged particle in three dimensions.

To avoid very strong signals produced by ions entering the chamber, a special gating electrode is mounted in front of the first GEM foil. Depending on the potential of this electrode, the ionization charge can be either attenuated (low-sensitivity mode) or fully transmitted to the amplification section (high-sensitivity mode). While waiting for a  ${}^6\text{He}$  bunches, the OTPC was kept in the low-sensitivity mode. The acquisition system was triggered by a signal from the REX facility, arriving 50 ms before the first macrobunch. The high-sensitivity mode was switched on 200 ms after the trigger, giving ample time for the implantation and for the removal of the large charge generated by  ${}^6\text{He}$  ions in the active volume. At the same time when the high sensitivity was switched on, the CCD exposure and the PMT waveform recording were started. In the beginning of the experiment the exposure time was set to 650 ms and the PMT signal was sampled with 100 MHz frequency. Later, the exposure time was extended to 880 ms and the sampling frequency was reduced to 50 MHz. After each exposure, the OTPC was switched back to the low-sensitivity mode and the event data (CCD image and the PMT waveform) were read and stored on a PC hard disk.

The OTPC was mounted in air just behind the beam-line vacuum window. The energy of incoming ions was just enough to traverse the vacuum window, the gap of air, and the thin windows protecting the active OTPC volume, to be finally

stopped inside the chamber. The kapton entrance window was covered with horizontal strips of  $5 \mu\text{m}$  of copper and  $2 \mu\text{m}$  of gold, which served as electrodes helping to maintain the uniform electric field in the chamber. The strips were 7 mm wide with 3 mm space between them. The beam spot was broader than one strip and 75% of ions that passed through such a strip lost more energy and were stopped at the depth of 7.6 cm in the active volume. The remaining 25% of ions were passing through a thinner layer and were stopped at the depth of 21.3 cm.

The atmospheric pressure in the Geneva region at the height of the laboratory and at the time of experiment was  $(97.0 \pm 0.5)$  kPa. The temperature in the laboratory was  $(22 \pm 2)^\circ\text{C}$ . The resulting density of the counting gas mixture was  $\rho = 0.177 \pm 0.002 \text{ mg/cm}^3$ .

Drift velocity in the gas mixture was established by observation of  $\alpha$  particle tracks, which vertically punched through the whole active volume of the chamber. Such particles were emitted by nuclides from natural radioactivity chains present in the walls of the device. During the experiment 26 such tracks were observed. Their span on the PMT waveform corresponds to the well-known vertical dimension of the chamber. Analysis of these tracks yielded the average value  $v_d = (6.2 \pm 0.1) \text{ mm}/\mu\text{s}$ .

Each GEM foil consisted of four electrically disconnected sections separated by 1 mm wide inactive strips. As the drifting electrons were not multiplied at the location of these strips, the corresponding dark lines were clearly visible on CCD images. Comparison of the distance between the lines on the image with the distance between the strips on the GEM foils provided the calibration coefficient for the length on the image plane. It was found that one pixel of the CCD image corresponds to  $(0.635 \pm 0.005) \text{ mm}$ .

### III. DATA ANALYSIS AND RESULTS

In 106 hours of data taking about 120 000 cycles of  ${}^6\text{He}$ , implantations into the OTPC detector were executed and the data set for each of them was taken and stored. The CCD images in most of them contained only a weak background due to  $\beta$  particles. Although the ionization signal from electrons is much weaker than from heavy charged particles, the large number of electrons emitted during the exposure produced a visible pattern of two clouds of light centered on the two locations where  ${}^6\text{He}$  ions were stopped. This is the result of the fact that the CCD camera is integrating all the light emitted during the exposure. In contrast, the  $\beta$  background is almost not visible on the PMT waveform, because the  $\beta$  decay events are distributed statistically over the whole exposure time. When a track of a heavy charged particle was present during the exposure, it produced a much stronger signal, clearly visible on the  $\beta$  background in the CCD image and in the PMT waveform. An example of a data set collected for one cycle of  ${}^6\text{He}$  implantation is shown in Fig. 1.

In the first step of data reduction only the data sets were selected that pictured such a strong signal. This was done by requiring that the amplitude of the PMT waveform exceeds a given threshold. To avoid rejecting low-energy events, the level of this threshold was set as low as possible, just above

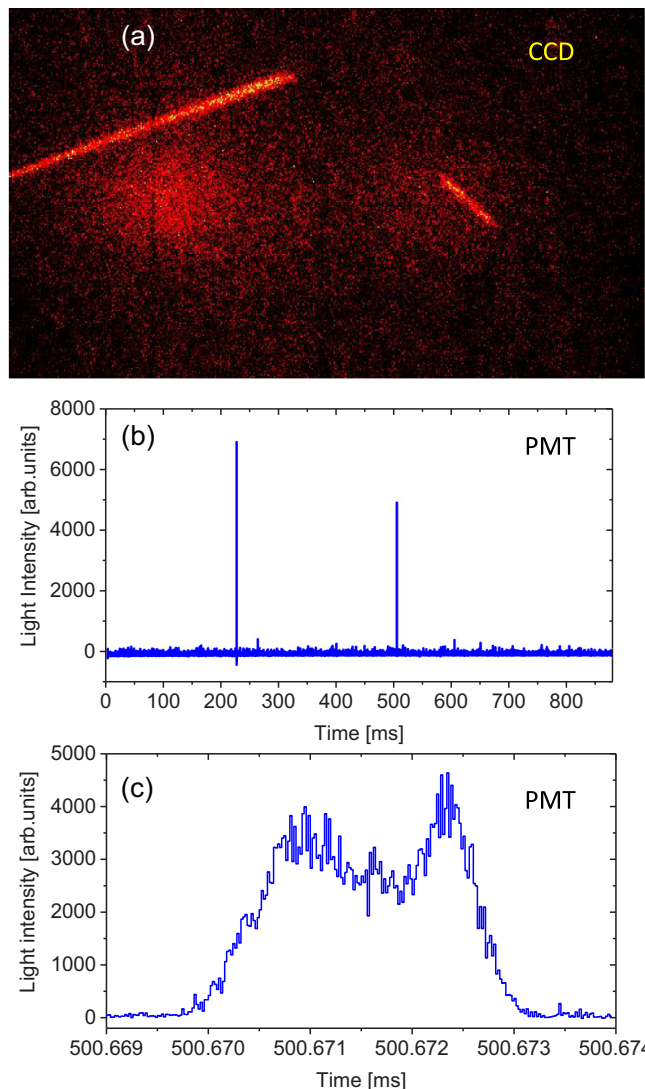


FIG. 1. (Color online) An example of one data set collected after implantation of  ${}^6\text{He}$ . (a) CCD image taken in 880 ms exposure,  ${}^6\text{He}$  ions entered from the left. On the smeared background due to  $\beta$  particles, two tracks are visible. The long one is an  $\alpha$  particle from natural background and the short one represents a decay of  ${}^6\text{He}$  into  $\alpha + d$ . (b) Full PMT waveform showing the light distribution over the entire exposure on which two events are seen. (c) Zoom on the waveform part around the second event showing the characteristic pattern of an  $\alpha$  particle (right) and a deuteron (left) emitted from the common origin in opposite direction.

the noise of the PMT signal. This procedure identified about 32 000 events for further analysis. Most of them contained only signals from  $\alpha$  particles emitted by natural radionuclides present in the walls of the detector. All of them were inspected individually and about 2000 events were identified as candidates for  $\beta d$  decay of  ${}^6\text{He}$  and were subjected to the energy reconstruction procedure. We have verified that for all these events, in particular for those of the lowest energy, the maximal amplitude of the PMT waveform exceeded the selection threshold at least by a factor of two. This assures that no low-energy events were rejected by the adopted selection.



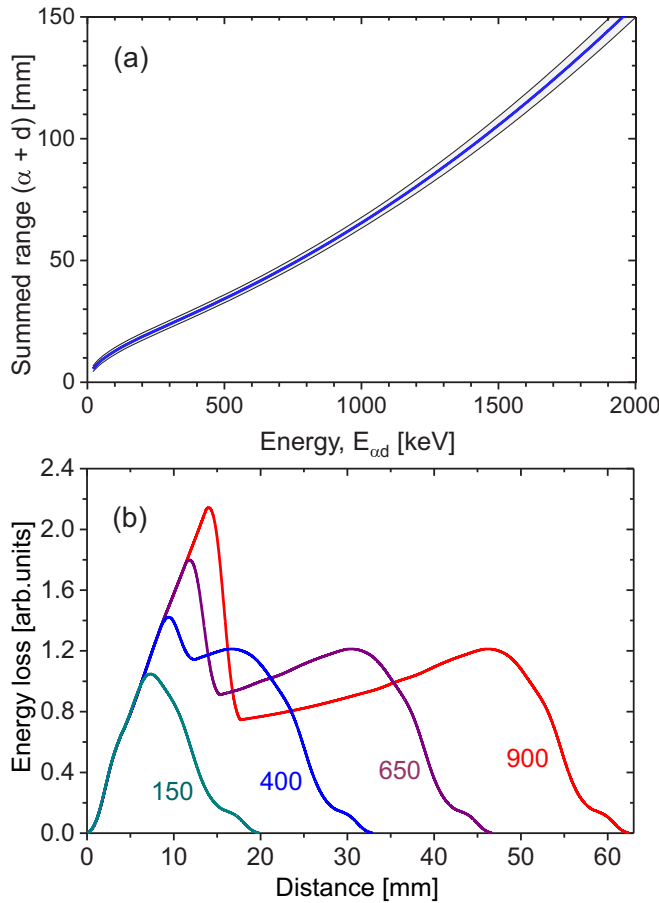


FIG. 2. (Color online) Results of SRIM calculations for the OTPC gas mixture. (a) Summed range of an  $\alpha$  particle and a deuteron as a function of  $(\alpha + d)$  energy  $E_{\alpha d}$ . The gray band illustrates the spread due to the range straggling. (b) Energy-loss profiles along the common track of the  $\alpha$  particle and the deuteron. The distance is measured from the end of the  $\alpha$  particle track. Four tracks are labeled by the energy  $E_{\alpha d}$  in keV.

Since the electron and the antineutrino emitted in the decay carry very small momentum, we can assume to a very good approximation that the deuteron and the  $\alpha$  particle, when emitted from the resting  ${}^6\text{He}$  atom, are moving in opposite directions with the kinetic energies inversely proportional to their masses. Thus, if the summed energy of both particles is  $E_{\alpha d}$ , the deuteron energy is  $E_d = (2/3)E_{\alpha d}$ , and the rest is taken by the  $\alpha$  particle. The reconstruction of the energy  $E_{\alpha d}$  was done essentially by comparing the measured total length of the track left by the  $\alpha$  particle and the deuteron with the simulation based on the SRIM2013 code [22]. First, the ranges of the  $\alpha$  particle and the deuteron in the gas mixture used in the experiment, as a function of their energies, were calculated. Then, the summed length of both particles as a function of the  $\alpha + d$  energy  $E_{\alpha d}$  was established, see Fig. 2 (top). Using the range functions of both particles, a profile of energy-loss distribution along the common track could be calculated. To take into account the diffusion of the primary ionization charges during the drift to the amplification zone, the profiles predicted by SRIM were folded with the normal (Gaussian)

distribution. The variance of this distribution,  $\sigma = 1.9$  mm, was found to describe well the observed tracks. Examples of such profiles are shown in Fig. 2 (bottom).

For each  $\alpha + d$  track the OTPC provided its vertical (PMT) and horizontal (CCD) components. Since the PMT signals had practically no background, the observed vertical components showed very clearly the projection of the energy-loss profiles of the track on the vertical axis (see Fig. 1, bottom). The horizontal projection of this profile was less clearly seen on the CCD image, mainly because of the integrated background due to  $\beta$  particles. The length of the horizontal projection, however, could be determined from the image with a good accuracy. In the energy reconstruction procedure, first the length of the horizontal component was determined from the CCD image. Then, the shape of the PMT waveform representing the vertical component was fitted with the energy-loss profile, as predicted by SRIM and projected on the vertical axis. The fitting parameters were the length of the vertical component and the overall normalization factor. From the two components the total length of the track was calculated and using the energy-range function the energy  $E_{\alpha d}$  was determined. Examples of events illustrating this procedure are presented in Fig. 3.

The reconstruction procedure identified about 1800  $\beta d$  events fully contained in the active volume, yielding the decay energy values and emission angles. It was observed

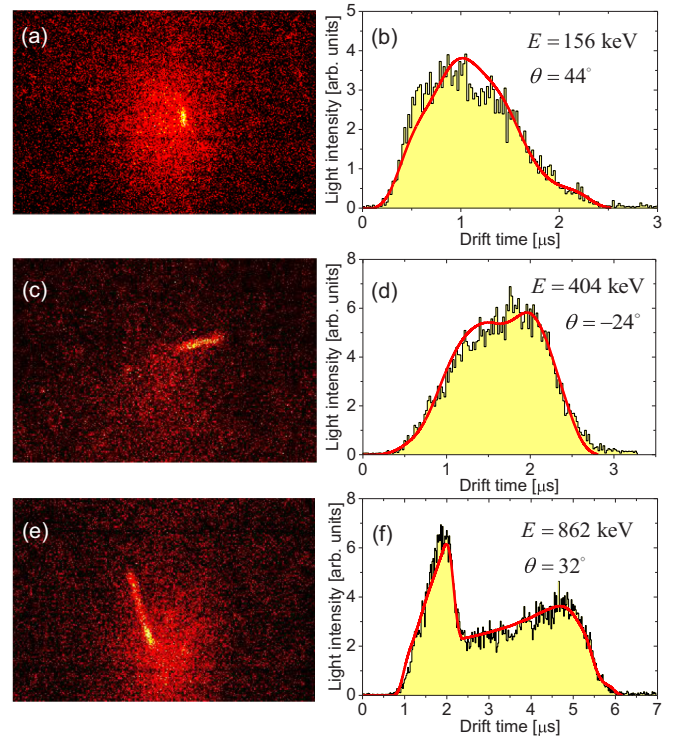


FIG. 3. (Color online) Examples of  ${}^6\text{He}$  decay into  $(\alpha + d)$  for the  $E_{\alpha d}$  energy of (a), (b) 156 keV, (c), (d) 404 keV, and (e), (f) 862 keV. For each event the relevant part of the CCD image is presented on the left, while the corresponding PMT waveform is shown on the right as a yellow histogram together with the best-fitted SRIM simulation represented by the solid (red) line. The angle  $\theta$  of the deuteron emission with respect to the horizontal plane is indicated. Each CCD image represents the same area.

that the normalization factor, representing the ratio between the recorded intensity of light and the SRIM prediction, showed strong fluctuations for the events with the lowest decay energies. We have concluded that the safe lower limit for the  $E_{\alpha d}$  value, for which our energy reconstruction is still reliable, is 150 keV, corresponding to the deuteron energy of 100 keV. Adopting this limit we have discarded about 90 events of lower energy. Furthermore, we have applied a condition that the decay occurs within 50 mm from one of the implantation centers, removing about 50 decays close to the walls of the chamber. Finally, this yielded 1651 well-identified and reconstructed  $\beta d$  decay events of  ${}^6\text{He}$ . In principle the uncertainty introduced by the reconstruction procedure is different for each event. We have found, however, that the value of 15 keV is a good measure for the standard deviation of the energy in the whole spectrum due to this procedure. Larger inaccuracy arises from the range straggling of particles in the gas. The effect of the straggling on the range of the  $\alpha + d$  track as a function of the energy  $E_{\alpha d}$  was calculated with the SRIM code, see Fig. 2. From this, the energy spread for a given range can be determined. The resulting energy inaccuracy is about 25 keV for  $E_{\alpha d} = 150$  keV, about 30 keV for  $E_{\alpha d}$  energies between 200 keV and 1000 keV, and then increases to about 40 keV at  $E_{\alpha d} = 1600$  keV. In addition, there is a systematical uncertainty related to the inaccuracy of the gas density. It grows from about 5 keV at energy  $E_{\alpha d} = 200$  keV, through 8 keV at  $E_{\alpha d} = 500$  keV, to 10 keV at  $E_{\alpha d} = 900$  keV.

The position distribution of the decay events on the horizontal (CCD image) plane is shown in Fig. 4. Two groups centered on the two implantation points are seen. Shapes of these distributions, both in the direction perpendicular to the beam axis ( $x$ ) and in the direction along the beam ( $z$ ), can be well approximated by Gaussian functions. Taking into account these observed distributions and the dimensions of the active volume of the chamber, we have made Monte Carlo simulations of the probability that a  $\alpha + d$  track of a given decay energy is fully contained within the active volume. Although we did not observe the vertical position distribution, it is constrained by the vertical size of the entrance window (3 cm) and in addition by the fraction of ions that passed through the thicker strip on this window. We found that different assumptions on the vertical distribution fulfilling these constraints lead to almost identical results. The adopted detector efficiency curve is presented in Fig. 5. It can be seen that up to the energy  $E_{\alpha d} = 1$  MeV all events are contained within the chamber and no efficiency corrections are needed.

Since we could not determine precisely the number of  ${}^6\text{He}$  ions implanted into the OTPC, we cannot determine the absolute decay probability from our data. Instead we use the results of Raabe *et al.* [8], who achieved the most precise value of the branching ratio, for normalization of our energy spectrum. First, we produced the histogram of our data points with exactly the same energy bins (100 keV wide) as shown in Fig. 3 of Ref. [8]. For the comparison we took only the data between 400 keV and 1000 keV. The former limit is the lowest energy observed in Ref. [8], the latter is the highest energy of our spectrum without any efficiency corrections. Then, the normalization factor has been determined, taking into account statistical errors of both spectra. Finally, we

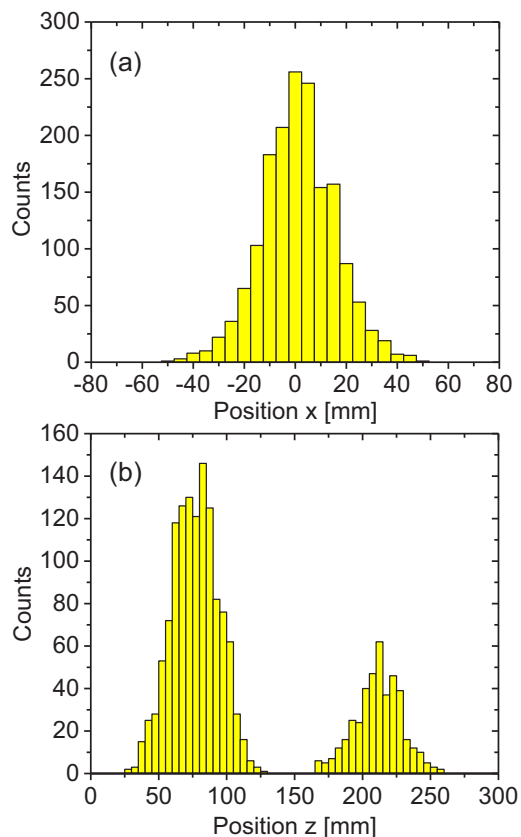


FIG. 4. (Color online) Position distribution of the  ${}^6\text{He}$  decay events on the horizontal plane. (a) Position in the direction perpendicular to the beam direction. The value of 0 corresponds to the beam axis. (b) Position in the direction along the beam axis.

present our spectrum as a histogram of 50 keV-wide energy bins starting from  $E_{\alpha d} = 150$  keV. The result, after the normalization and the correction for the OTPC efficiency, is shown in Fig. 6. By integrating the whole spectrum the total branching ratio for the  $\alpha + d$  decay of  ${}^6\text{He}$ , for the deuteron energy larger than 100 keV, is found to be  $B = [2.78 \pm 0.07(\text{stat}) \pm 0.17(\text{sys})] \times 10^{-6}$ , where the first uncertainty is the statistical one and the second represents the inaccuracy of the normalization. From this value the transition probability can be deduced using the relation  $W = B \ln 2 / T_{1/2}$ . The result is  $W = [2.39 \pm 0.06(\text{stat}) \pm 0.15(\text{sys})] \times 10^{-6} \text{ s}^{-1}$ . Thus, our value is about 70% larger than the intensity measured by Raabe *et al.* [8]. The difference is made by the spectrum below the energy threshold of  $E_{\alpha d} = 525$  keV, corresponding to the deuteron energy of 350 keV, which was the limit in the previous experiments [7,8].

In Fig. 6 the experimental data are compared with the prediction of the three-body model by Tursunov *et al.* [15]. We show the result of calculations assuming a simple Gaussian attractive potential for the  $\alpha + d$  system in the final state ( $V_m$  from Ref. [15]). This version was found to best reproduce the experimental result of Ref. [7]. The shape of the predicted spectrum is in good agreement with experiment in the full energy range. The integrated transition probability, for the deuteron energy larger than 100 keV, according to this model is

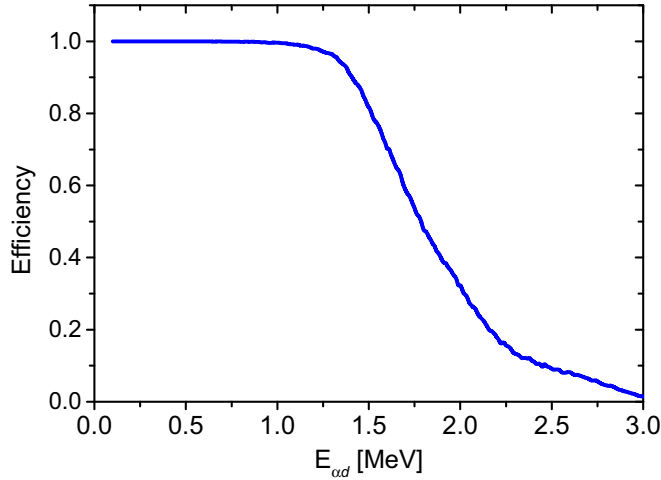


FIG. 5. (Color online) The OTPC efficiency curve for the present experiment defined as the probability that the full ( $\alpha + d$ ) track will be contained in the OTPC active volume, as a function of the ( $\alpha + d$ ) energy  $E_{\alpha d}$ .

$W_{th} = 2.01 \times 10^{-6} \text{ s}^{-1}$ . Thus, the predicted intensity is about 20% smaller than the result of our measurement.

#### IV. SUMMARY

We have measured the very weak branch of  $\beta$  decay of  ${}^6\text{He}$  into an  $\alpha$  particle and a deuteron. The ions of  ${}^6\text{He}$  were produced, separated, and postaccelerated at the REX-ISOLDE facility and implanted into a gaseous detector—the optical time projection chamber. This detector allowed us to record tracks of  $\alpha + d$  particles in three dimensions and to reconstruct the sum of their energies  $E_{\alpha d}$ . Due to the very low sensitivity of

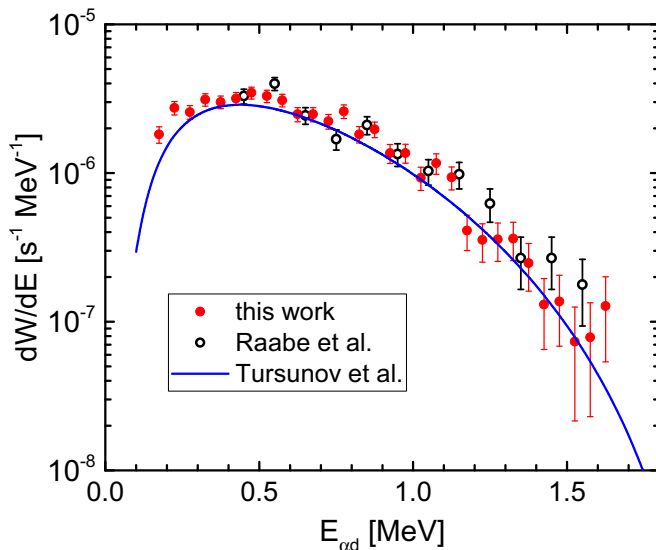


FIG. 6. (Color online) Transition probability of the  $\alpha + d$  branch in the  $\beta$  decay of  ${}^6\text{He}$  as a function of the ( $\alpha + d$ ) energy  $E_{\alpha d}$ . The results of this work are shown by the solid points while the open points are from Ref. [8]. The solid line represents the prediction from the Ref. [15].

the OTPC to  $\beta$  electrons, we were able to investigate this exotic decay for the energies  $E_{\alpha d}$  below 525 keV, corresponding to the deuteron energy of 350 keV, which was the limit of the previous experiments [7,8]. In the data analysis, we could successfully reconstruct 1651  $\alpha + d$  events extending the spectrum down to the energy  $E_{\alpha d} = 150$  keV, corresponding to the deuteron energy of 100 keV. The shape of our spectrum, for the energy  $E_{\alpha d} > 525$  keV, agrees well with the results obtained previously.

For the absolute normalization we have taken the data of Raabe *et al.* [8] as the reference. The normalization factor was determined by comparing the transition probability distribution established in Ref. [8] with our spectrum in the energy range between 400 and 1000 keV. This allowed to calculate the total branching ratio for the  $\beta d$  channel in  ${}^6\text{He}$  for the energy  $E_{\alpha d} \geq 150$  keV to be  $B = [2.78 \pm 0.07(\text{stat}) \pm 0.17(\text{sys})] \times 10^{-6}$ , which corresponds to the total transition probability  $W = [2.39 \pm 0.06(\text{stat}) \pm 0.15(\text{sys})] \times 10^{-6} \text{ s}^{-1}$ . Thus, the achieved extension of the spectrum to lower energies revealed about 70% more of the transition intensity.

The comparison with the theoretical three-body model of Tursunov *et al.* [15] showed that the shape of our spectrum is in a very good agreement with the prediction. This supports a requirement for the  ${}^6\text{He}$  ground-state wave function to have the correct three-body asymptotic behaviour, which is one of the key ingredients of the model. The measured total transition probability, however, is about 20% larger than the predicted one in the same energy range. The increase of the calculated intensity can be achieved, to some extent, by modifications of the scattering potential in the  $\alpha + d$  channel. This potential, however, is constrained by the known  ${}^6\text{Li}$  ground-state energy and by the measured  $\alpha + d$  phase shifts [15]. A new theoretical inquiry is needed to determine whether the observed discrepancy in the total transition probability can be removed by modifications of the  $\alpha + d$  interaction alone, or some improvements in the description of the  ${}^6\text{He}$  halo wave function have to be introduced.

We have demonstrated that a gaseous detector of the TPC type is a very efficient and sensitive tool for the study of decays with emission of heavy charged particles. This technique is particularly advantageous when low-energy particles have to be recorded in the presence of a large background from  $\beta$  electrons. In principle our method could be used to measure the  ${}^6\text{He}$   $\beta$ -delayed deuterons of even lower energies. Then, however, a gas mixture of lower density should be used, which could be achieved by maintaining a lower gas pressure in the detector active volume.

#### ACKNOWLEDGMENTS

We would like to thank the ISOLDE facility for providing the excellent beam. We are grateful to P. Descouvemont for providing us with the results of Ref. [15] in a tabular form. The work was partially supported by the Polish National Science Center under Contract No. UMO-2011/01/B/ST2/01943, by the European Nuclear Science and Applications Research (EN-SAR) under Project No. 262010, by the Research Foundation - Flanders (FWO), by GOA/2010/010 (BOF KU Leuven), and by the Interuniversity Attraction Poles Programme initiated by the Belgian Science Policy Office (BriX network P7/12).

- [1] K. Riisager, *Phys. Scr.*, T **152**, 014001 (2013).
- [2] A. S. Jensen, K. Riisager, D. V. Fedorov, and E. Garrido, *Rev. Mod. Phys.* **76**, 215 (2004).
- [3] K. Riisager *et al.*, *Phys. Lett. B* **235**, 30 (1990).
- [4] I. Mukha *et al.*, *Phys. Lett. B* **367**, 65 (1996).
- [5] D. R. Tilley *et al.*, *Nucl. Phys. A* **708**, 3 (2002).
- [6] M. J. G. Borge *et al.*, *Nucl. Phys. A* **560**, 664 (1993).
- [7] D. Anthony *et al.*, *Phys. Rev. C* **65**, 034310 (2002).
- [8] R. Raabe *et al.*, *Phys. Rev. C* **80**, 054307 (2009).
- [9] P. Descouvemont and C. Leclercq-Willain, *J. Phys. G* **18**, L99 (1992).
- [10] M. V. Zhukov, B. V. Danilin, L. V. Grigorenko, and N. B. Shul'gina, *Phys. Rev. C* **47**, 2937 (1993).
- [11] D. Baye, Y. Suzuki, and P. Descouvemont, *Prog. Theor. Phys.* **91**, 271 (1994).
- [12] K. Varga, Y. Suzuki, and Y. Ohbayasi, *Phys. Rev. C* **50**, 189 (1994).
- [13] A. Csóto and D. Baye, *Phys. Rev. C* **49**, 818 (1994).
- [14] F. C. Barker, *Phys. Lett. B* **322**, 17 (1994).
- [15] E. M. Tursunov, D. Baye, and P. Descouvemont, *Phys. Rev. C* **73**, 014303 (2006); **74**, 069904(E) (2006).
- [16] O. Kester *et al.*, *Nucl. Instrum. Methods Phys. Res., Sect. B* **204**, 20 (2003).
- [17] K. Miernik *et al.*, *Phys. Rev. Lett.* **99**, 192501 (2007).
- [18] M. Pomorski *et al.*, *Phys. Rev. C* **90**, 014311 (2014).
- [19] K. Miernik *et al.*, *Phys. Rev. C* **76**, 041304(R) (2007).
- [20] M. Pomorski *et al.*, *Phys. Rev. C* **83**, 014306 (2011).
- [21] F. Sauli, *Nucl. Instrum. Methods A* **580**, 971 (2007).
- [22] J. F. Ziegler, The Stopping and Range of Ions in Matter (SRIM), <http://www.srim.org>